UCRL--102793

DE90 008325

An Intercomparison of General Circulation Model Predictions of Regional Climate Change

Presented at the International Conference on
"Modelling of Global Climate Change and Variability"

Hamburg, Federal Republic of Germany
September, 1989

Stanley L. Grotch
Atmospheric and Geophysical Sciences Division
Lawrence Livermore National Laboratory
Livermore, California, USA
FAX: (415) 422-7675

Abstract

Simulations using the best-available general circulation models (GCMs) to estimate the sensitivity of the climate to a doubling of the atmospheric carbon dioxide concentration are in broad general agreement that, at equilibrium, the global annual average surface air temperature would increase about 2-5K. Because of considerable public interest in potential climate changes due to greenhouse gases, there is pressure to use the predictions of these GCM simulations for regional climate assessments. This requires more detailed evaluation of the agreement of the GCM predictions on smaller regional scales. In this work, statistical intercomparisons were made of the estimates for both the control (1 x CO_2) and the equilibrium changes in surface air temperature and precipitation after a doubling of atmospheric CO_2 as predicted by five GCMs: NCAR/CCM, GFDL, GISS, OSU, and the United Kingdom Meteorological Office (UKMO). Intercomparisons were also made with historical data for the simulations of current climate.

Although the results of these GCMs often agree well with each other and with historical data when averaged over large scales (global, hemispheric, zonal), if the model results are examined on successively smaller and smaller scales, as small as subcontinental regions containing only relatively few (10-100) gridpoints, significant differences arise.

It is apparent that if these simulations represent "state of the art" results, this art is not yet ready to be used for quantitative prediction on scales as small as subcontinental regions, let alone a single surrogate gridpoint representing a particular small area or city.

1. Introduction

In this study the question addressed is: "How well do the predictions of different GCMs agree with each other and with observational data at different spatial scales?" The basic answer to this question is that although the models often agree reasonably well in estimating larger scale averages, more detailed spatial agreement at regional scales below continental is generally poor.

Although model resolution appears adequate globally for the finest 4° latitude x 5° longitude resolution of the five models examined here, the difficulty faced in using model results at this resolution for smaller subcontinental regional scales such as, for example, Europe becomes apparent upon magnification (see Fig. 1).

Two data fields which are of particular importance in regional impacts studies are examined here: (1) surface air temperature and (2) precipitation. The seasonally averaged results predicted by five GCMs are intercompared among models and with observational data for the control climate over different scales. Intercomparisons are also made among the models for predictions of the change at equilibrium in these two variables after a doubling of atmospheric carbon dioxide.

These intercomparisons are made for these seasonally averaged variables in three different ways:

(1) Zonal medians of precipitation are intercompared (e.g., the median value of either temperature or precipitation at a given latitude). The median is used rather than the arithmetic average since it is a statistically more robust measure of location because it is less sensitive to the presence of any extreme values.

(2) The longitudinal distributions of precipitation at a fixed latitude are graphically intercompared. The five GCMs and two gridded observational data sets all have gridpoints located very close to 50°N latitude which traverses across densely populated and agriculturally important regions of the Northern Hemisphere.

(3) Model predictions for seasonally averaged surface air temperature are intercompared at individual gridpoints over the European land area from the Atlantic to the Urals and from southern Scandinavia to the Mediterranean.

Data from five published GCM studies of the equilibrium changes due to a doubling of CO_2 will be used here:

(1) CCM (Washington and Meehl, 1984)

(2) GFDL (Manabe and Wetherald, 1987)

(3) GISS (Hansen et al., 1984)

(4) OSU (Schlesinger and Zhao, 1989)

(5) UKMO (Wilson and Mitchell, 1987).

For observational surface air temperatures the gridded data of Oort (1983) and Schutz and Gates (1972) are used. The gridded precipitation data sets of Jaeger (1976) and Schutz and Gates (1972) are also used.

2. Zonal Predictions of Precipitation and Change in Precipitation

Figure 2 displays the zonal median values of seasonally averaged (Dec/Jan/Feb) precipitation (mm/day) for the control simulation (e.g., 1 x CO_2) for four GCMs (CCM, GFDL, GISS, OSU) and the observational data set of Jaeger. Although the models and historical data both show the same general distributions (e.g., a central peak near the equator and two lower peaks at about 50°S and 40°N), substantial percentage differences exist between the models and observation. Recall that the values plotted in Fig. 2 are the *median* values of from 36 to 72 individual longitudinal values at each latitude. Thus, as will be seen later, at individual longitudinal gridpoints *even greater differences* can occur.

Figure 3 displays comparable predictions for the change in Dec/Jan/Feb seasonally-averaged precipitation for the four GCMs. Although the globally-averaged changes are of comparable magnitude, there is poor quantitative agreement even in the latitudinal distribution of these average changes. This is also seen in Fig. 4, which superposes

seasonally-averaged median changes predicted by the four GCMs for Dec/Jan/Feb and June/July/August.

3. Longitudinal Distribution of Precipitation and Change in Precipitation

To intercompare model predictions and observational data on a finer scale, the longitudinal distribution of annually averaged precipitation along a cut at latitude 50°N was examined. This particular latitude was selected for two reasons: (1) the five GCMs and two gridded observational data sets of precipitation all have gridpoints within 3° of this latitude, (2) this transect passes across some of the most important population and agricultural centers of the Northern Hemisphere.

Figure 5 displays the longitudinal distributions for annually averaged control precipitation for the five GCMs and two observational gridded data sets (Jaeger, Schutz-Gates). The longitudinal distribution of the two observational sets agree quite well at this latitude as do several of the GCMs (see, for example Fig. 6 for an intercomparison of the CCM and GFDL results).

However, at still higher resolution, intercomparisons show substantial quantitative differences. For example, Figure 7 shows the GCM predictions for annual precipitation at 50°N latitude over European and Asian regions (0°E to 180°E) indicating very substantial differences over specific longitude ranges (often >100%). Even poorer agreement is found upon intercomparing the *percentage change* in annually averaged precipitation predicted after a doubling of CO_2 among the five GCMs over the same region (Fig. 8).

In model intercomparison studies one commonly examines zonally averaged behavior (as was done in the previous section of this work). It is particularly important, therefore, to emphasize the dangers than can result if one implicitly assumes that good agreement of zonal averages necessarily implies good agreement on finer longitudinal

scales. Consider the following example taken from these model predictions for the percentage change in annual precipitation at 50°N latitude. The zonally averaged percentage changes after a doubling of CO_2 predicted by the CCM and UKMO models are 24.5% and 26.0%, respectively, suggesting rather close agreement. However, as shown in Figure 9 where the detailed longitudinal distributions at 50°N for these two models are displayed, excellent agreement of the averages can hide very much larger regional differences.

4. Surface Temperature Intercomparisons over the Land Areas of Europe

In impact studies of potential greenhouse warming, subcontinental areas are usually considered. Model and observational data are intercompared for seasonally averaged surface air temperature over the land area of Europe bounded approximately by the Atlantic to the east and the Urals to the west, southern Scandinavia to the north, and the Mediterranean to the south. (More specifically: 10°W to 60°E longitude and 40°N to 60°N latitude, see Fig. 10). Model and observational temperature data were first separately interpolated using bicubic splines to a common 4° latitude x 5° longitude grid. At this resolution, this land area contained 52 gridpoints.

Fig. 11 compares the two observational data sets of Oort and Schultz-Gates for Dec/Jan/Feb and June/July/August. Each of the 52 points in each subplot is an individual land-based gridpoint in the area defined in Fig. 10. The agreement between the two observational data sets is excellent with correlations of 0.99 and 0.96 for the two seasons. Similar results for Dec/Jan/Feb for the lowest and the highest GCM correlations with respect to the Oort observational data are displayed n Fig. 12. The correlations in this intercomparison are still high, ranging from 0.87 to 0.97. Similarly, the pairwise correlations between all five models for Dec/Jan/Feb is excellent, ranging from 0.91 to 0.98. However, these results degrade significantly in the June/July/August season where

the model to Oort correlations range from 0.56 to 0.91 and the between model correlations vary from 0.03 to 0.91.

Comparable intercomparisons may be made using the GCM predictions for the change in seasonally averaged surface air temperature after a doubling of CO_2. These results are strikingly poorer, particularly for the June/July/August predictions. The lowest and highest cross correlations for Dec/Jan/Feb predicted change in temperature for the five GCMs are displayed in Fig. 13. Here, even the best correlation case (0.84) clearly indicates poor quantitative agreement at the gridpoint level between these models over this area. The June/July/August results are even poorer; for 6 of the 10 pairwise intercomparisons, the cross correlations between models are *negative* with the *highest* cross correlation is only 0.3.

These calculations have been repeated over a number of Northern Hemisphere areas with generally similar results: (a) seasonally averaged control temperatures are generally reasonably well predicted for Dec/Jan/Feb, somewhat less so for June/July/August; (b) correlations among GCMs at the gridpoint level for changes in temperature due to doubling CO_2 are generally poor for Dec/Jan/Feb and non-existent for June/July/Aug.

5. Conclusions

These results strongly suggest that the results from GCM simulations are still not consistent enough to be used for quantitative predictions on anything approaching the scale of several (approximately 10-100) gridpoints. This poses a dilemma for those regional planners who would wish to use these results *now* for smaller sub-continental, national or local studies.

One cause of the different estimates of regional and seasonal sensitivity to a doubled CO_2 concentration is almost certainly related to the limitations in the quality of model

simulations of the present climate. Improvement of sensitivity estimates will, therefore, require a sustained effort to improve the climate models and investigations to determine the theoretical limits of the various time and space scales of climate predictability. Many uncertainties are also apparent in the model simulations of the present climate, indicating that further model improvements are needed to achieve reliable regional and seasonal projections of the future climatic conditions.

Acknowledgement

This work was sponsored by the U.S. Department of Energy Atmospheric and Climate Research Division and performed by the Lawrence Livermore National Laboratory under Contract No. W-7405-Eng-48.

References

Hansen, J., Lacis, A., Rind, D., Russel, G., Stone, P., Fung, I., Ruedy, R., and Lerner, J. (1984). Climate Sensitivity: Analysis of Feedback Mechanisms, 130-163. J. E. Hansen and T. Takahashi (eds.) Climate Processes and Climate Sensitivity, (Maurice Ewing Series, No. 5) American Geophysical Union Washington DC pp 368.

Jaeger, L., (1976). Monatskarten des Niederschlags für die ganze Erde Berickte des Deutschen Wetterdienstes, 139:1-38.

Manabe, S. and Wetherald, R. T. (1986). Reduction in Summer Soil Wetness Induced by an Increase in Atmospheric Carbon Dioxide. Science, 232:626-628.

Manabe, S. and Wetherald, R. T. (1987). Large Scale Changes of Soil Wetness Induced by an Increase in Atmospheric Carbon Dioxide. J. Atmos. Sciences, 44:1211-1235.

Oort, A. H. (1983). Global Atmospheric Circulation Statistics 1958-1973. NOAA Professional Paper 14 U.S. Govt. Printing Office, Washington, DC.

Schlesinger, M. E. and Zhao, Z. C., (1989). Seasonal Climatic Changes Induced by Doubled CO_2 as Simulated by the OSU Atmospheric GCM/Mixed-layer Ocean Model. J. of Climate, 2:459-495.

Schutz, C. and Gates, W. L. (1972). Global Climatic Data for Surface, 800 mb 400 mb July Report R-1029-ARPA Rand Corporation, Santa Monica, California. Available from NTIS (AD-760283), Springfield, VA.

Schutz, C. and Gates, W. L. (1972). Global Climatic Data for Surface, 800 mb 400 mb January Report R-915-ARPA Rand Corporation, Santa Monica, California. Available from NTIS (AD-760283), Springfield, VA, 1971.

Washington, W. M. and Meehl, G. A. (1983). General Circulation Model Experiments on the Climatic Effects Due to a Doubling and Quadrupling of Carbon Dioxide Concentrations. J. Geophys. Research, 88:6600-6610.

Washington, W. M. and Meehl, G. A. (1984). Seasonal Cycle Experiment on the Climate Sensitivity Due to a Doubling of CO_2 with an Atmospheric General Circulation Model Coupled to a Simple Mixed-Layer Ocean Model. J. of Geophys. Research, 89:9475-9503.

Wilson, C. A. and Mitchell, J. F. B. (1987). A Doubled CO_2 Climate Sensitivity Experiment with a Global Climate Model Including a Simple Ocean. J. of Geophysical Research, 92:13315-13343.

Figures

Figure 1. Global and European maps showing the boundaries of a 4° latitude by 5° longitude grid. The darkened area at the center of each grid is 1° latitude by 1° longitude.

Figure 2. Zonal median values for seasonally averaged Dec/Jan/Feb precipitation (mm/day) for 4 GCMs and the Jaeger observational data set (heavy curve).

Figure 3. Individual zonal median values for seasonally averaged Dec/Jan/Feb change in precipitation (mm/day) after a doubling of CO_2 for four GCMs.

Figure 4. Superposed zonal median values for seasonally averaged Dec/Jan/Feb and June/July/August changes in precipitation (mm/day) after a doubling of CO_2 for four GCMs.

Figure 5. Longitudinal distributions of annually averaged control precipitation predicted by five GCMs and two observational data sets at approximately 50°N latitude. (All subplots are to the same scale: 0 to 6 mm/day).

Figure 6. Longitudinal distributions of annually averaged control precipitation predicted by the CCM and GFDL GCMs at approximately 50°N latitude.

Figure 7. Longitudinal distributions of annually averaged control precipitation predicted by five GCMs at approximately 50°N latitude and longitudes from 0°E to 180°E.

Figure 8. Longitudinal distributions of the predicted percentage change in annually averaged precipitation after a doubling of CO_2 as predicted by five GCMs at approximately 50°N latitude and longitudes from 0° to 180°E.

Figure 9. Longitudinal distributions of the percentage changes in annually averaged precipitation after a doubling of CO_2 predicted by the GCM and UK Met Office GCMs at approximately 50°N latitude. Although the zonally averaged changes are virtually identical (24.5% and 26.0%) at this latitude, substantially larger regional differences arise.

Figure 10. The area of Europe used in the regional gridpoint intercomparison study. At a 4° latitude by 5° longitude resolution, 52 land-based gridpoints are contained in this region.

Figure 11. Seasonally averaged Dec/Jan/Feb and June/July/August temperatures from the observational data sets of Oort and Schutz and Gates. Each of the 52 points in each subplot is an individual land-based gridpoint in the area defined in Fig. 10.

Figure 12. The lowest and the highest correlated GCM results for seasonally averaged Dec/Jan/Feb temperatures from the five GCMs and the observational data set of Oort. Each of the 52 points in each subplot is an individual land-based gridpoint in the area defined in Fig. 10.

Figure 13. The lowest and the highest correlated pair of GCM results for seasonally averaged change in Dec/Jan/Feb temperatures from the five GCMs. Each of the 52 points in each subplot is the model prediction for change in temperature at an individual land-based gridpoint in the area defined in Fig. 10.

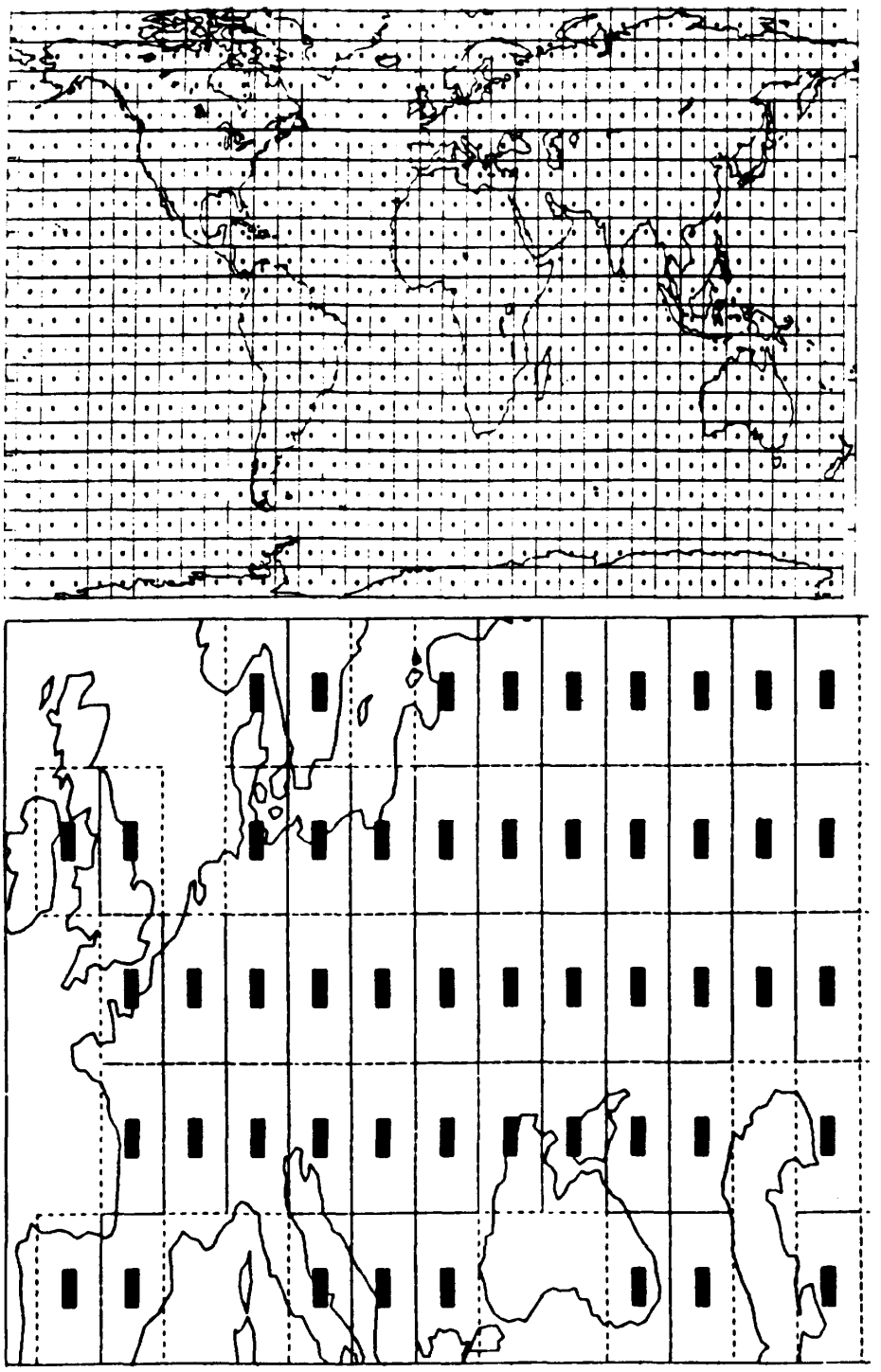

Figure 1. Global and European maps showing the boundaries of a 4° latitude by 5° longitude grid. The darkened area at the center of each grid is 1° latitude by 1° longitude.

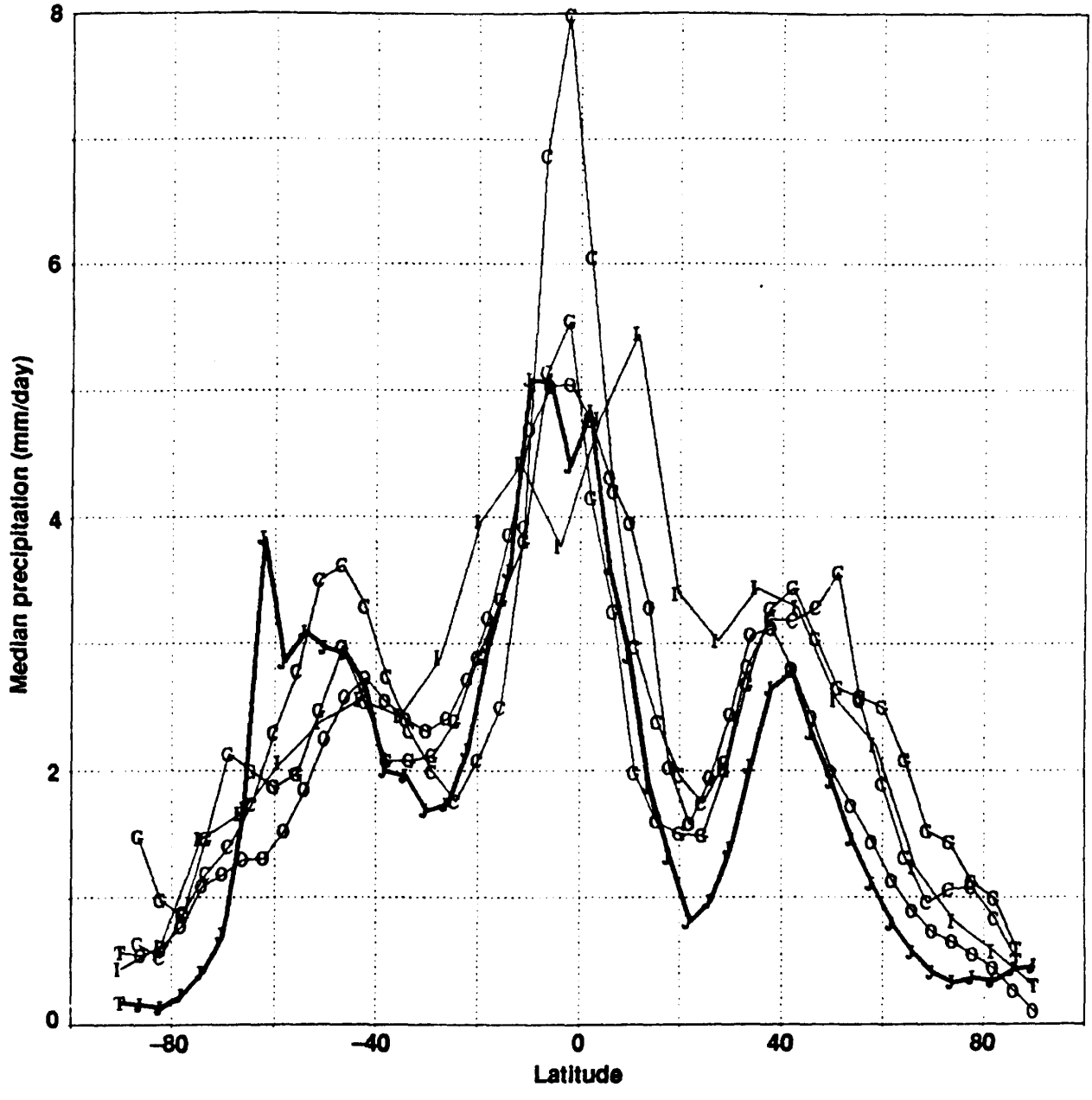

Figure 2. Zonal median values for seasonally averaged Dec/Jan/Feb precipitation (mm/day) for 4 GCMs and the Jaeger observational data set (heavy curve).

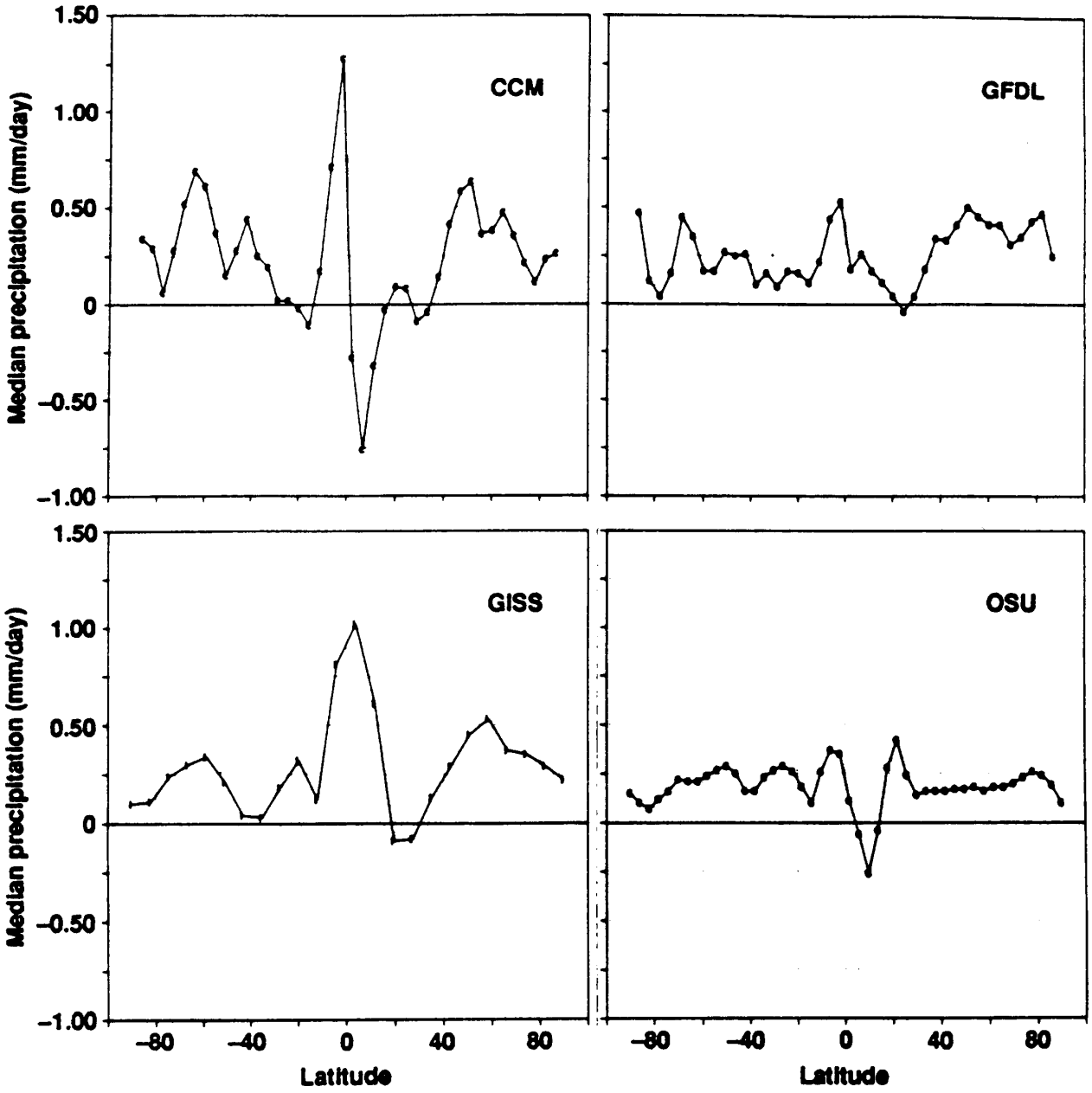

Figure 3. Individual zonal median values for seasonally averaged Dec/Jan/Feb change in precipitation (mm/day) after a doubling of CO_2 for four GCMs.

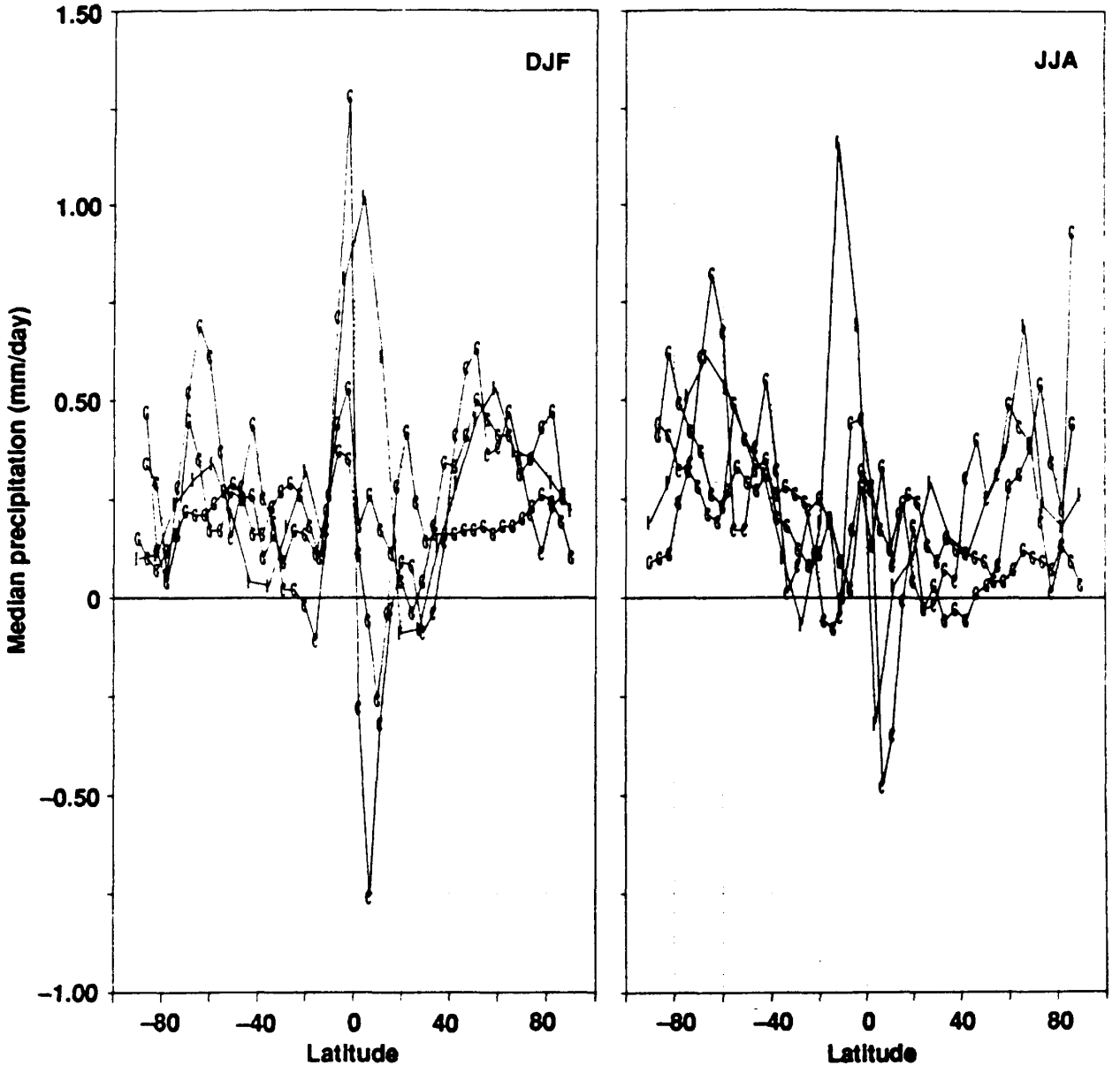

Figure 4. Superposed zonal median values for seasonally averaged Dec/Jan/Feb and June/July/August changes in precipitation (mm/day) after a doubling of CO_2 for four GCMs.

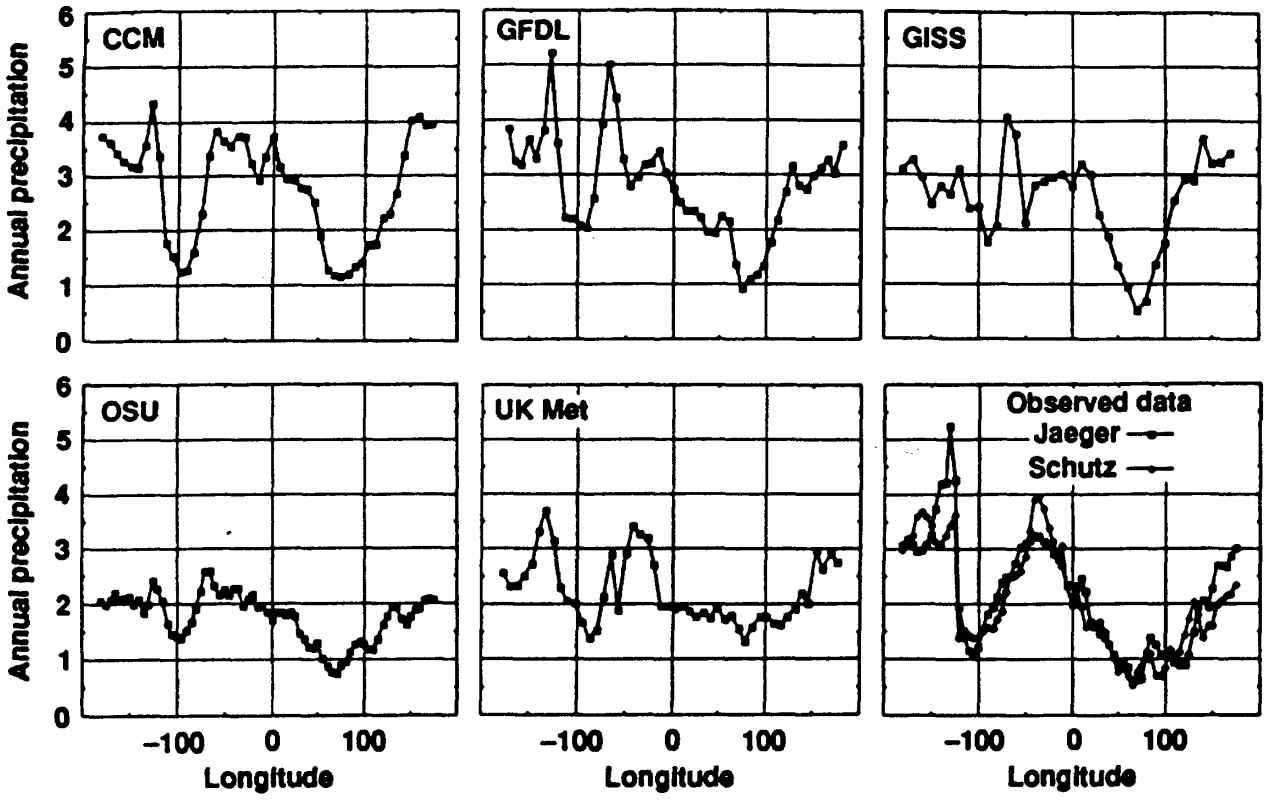

Figure 5. Longitudinal distributions of annually averaged control precipitation predicted by five GCMs and two observational data sets at approximately 50° N latitude. (All subplots are to the same scale: 0 to 6 mm/day).

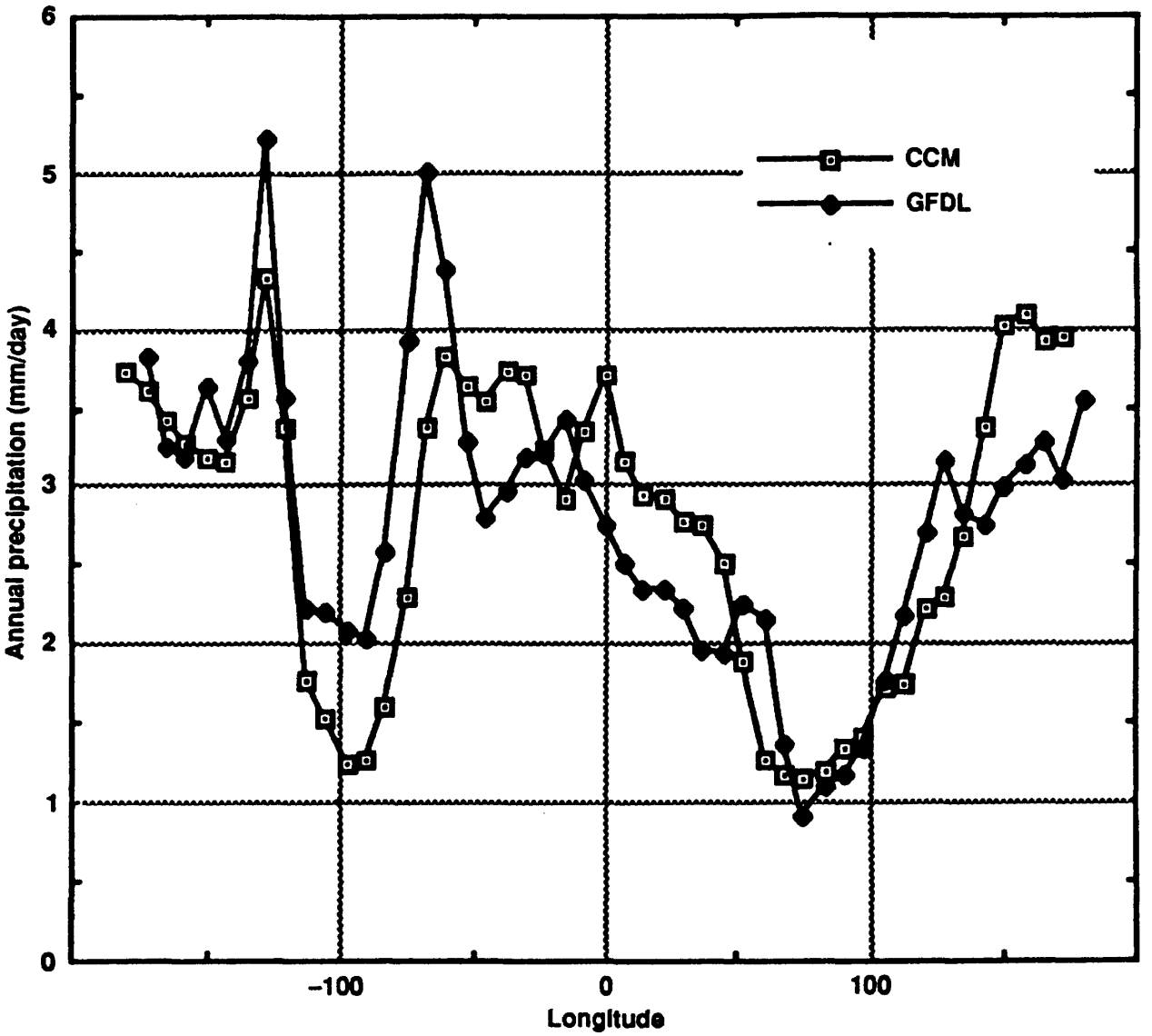

Figure 6. Longitudinal distributions of annually averaged control precipitation predicted by the CCM and GFDL GCMs at approximately 50° N latitude.

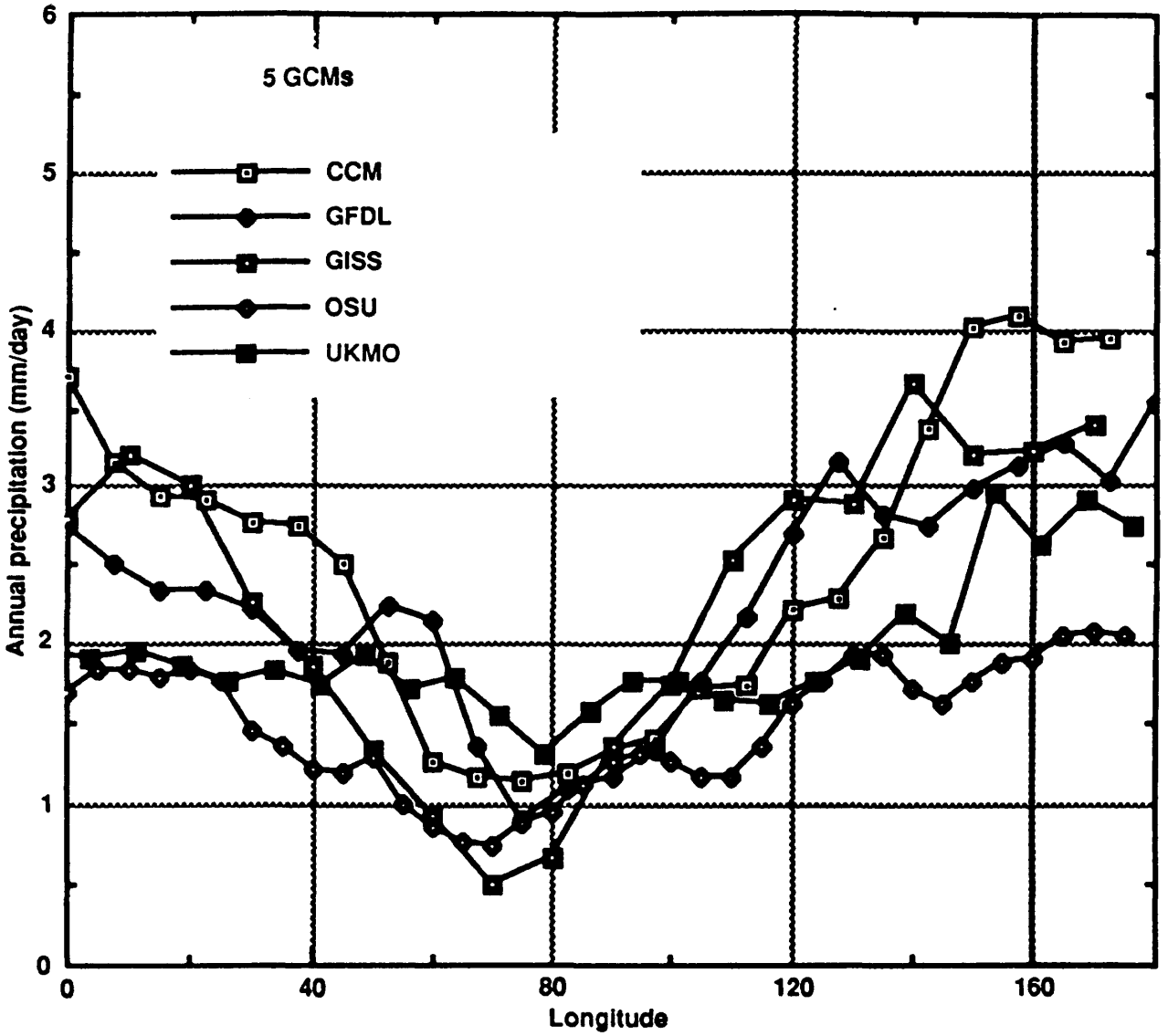

Figure 7. Longitudinal distributions of annually averaged control precipitation predicted by five GCMs at approximately 50° N latitude and longitudes from 0° to 180° E.

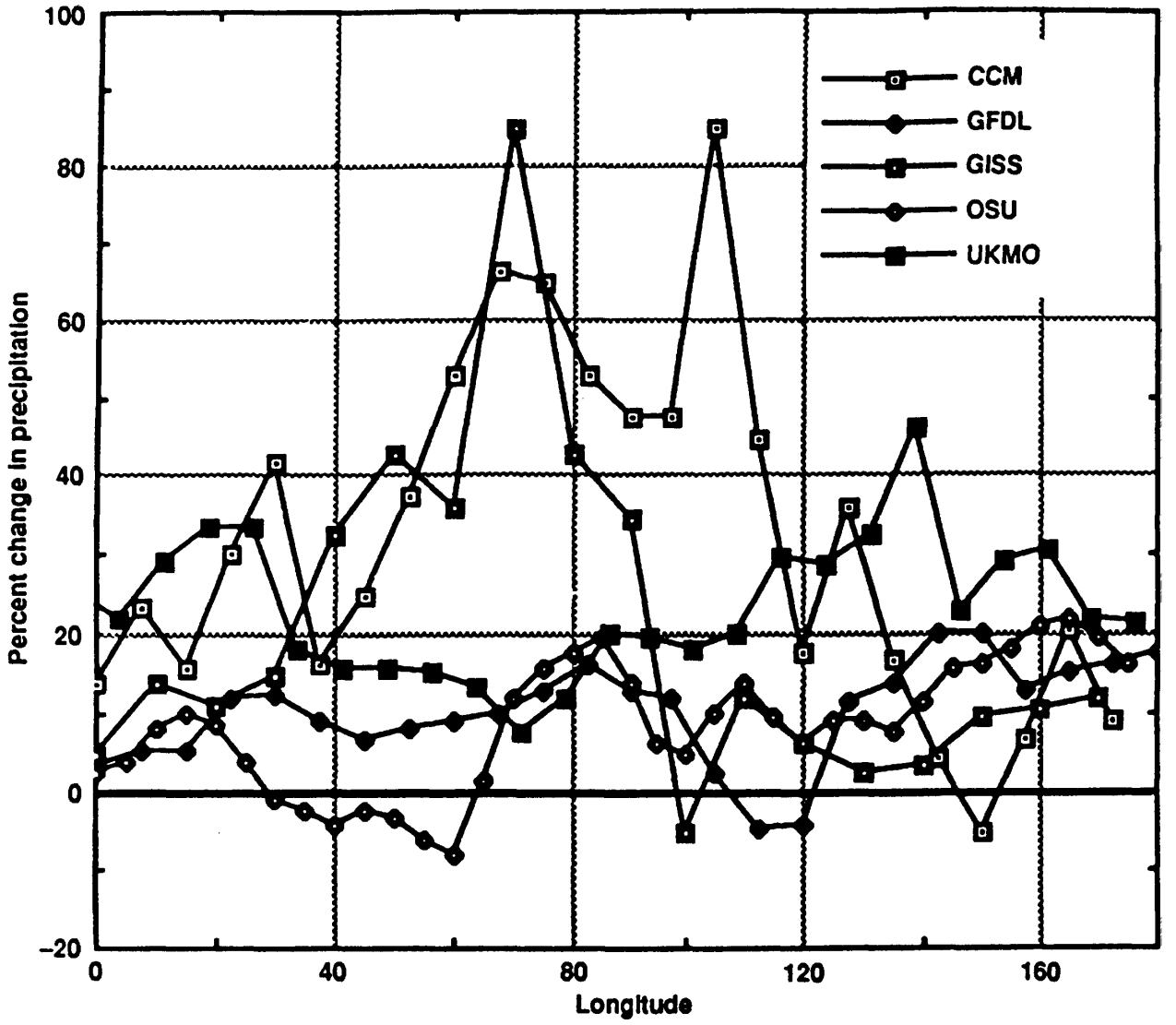

Figure 8. Longitudinal distributions of the predicted percentage change in annually averaged precipitation after a doubling of CO_2 as predicted by five GCMs at approximately 50° N latitude and longitudes from 0° to 180° E.

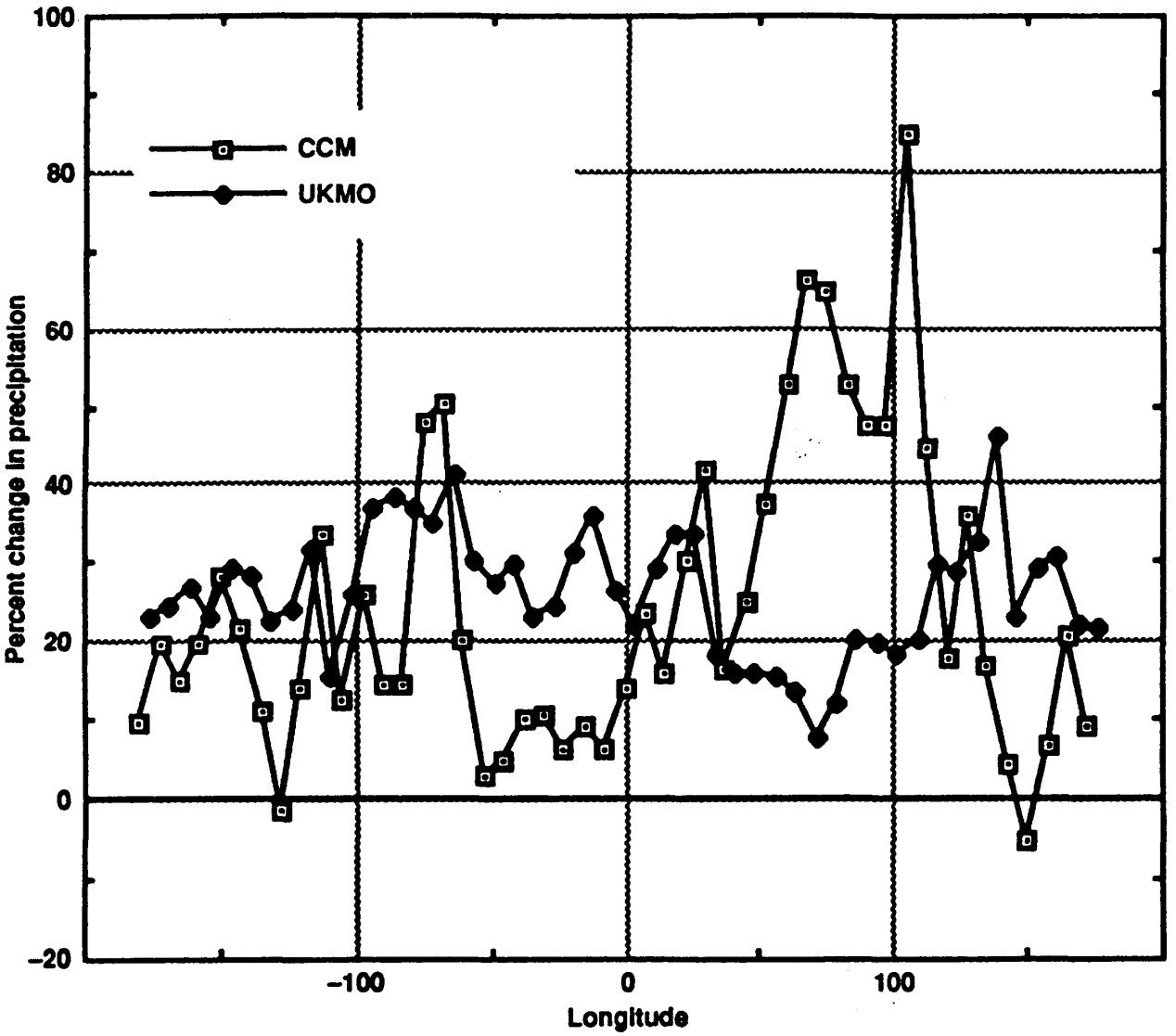

Figure 9. Longitudinal distributions of the percentage changes in annually averaged precipitation after a doubling of CO_2 predicted by the CCM and UK Met Office GCMs at approximately 50° N latitude. Although the zonally averaged changes are virtually identical (24.5% and 26.0%) at this latitude, substantially larger regional differences arise.

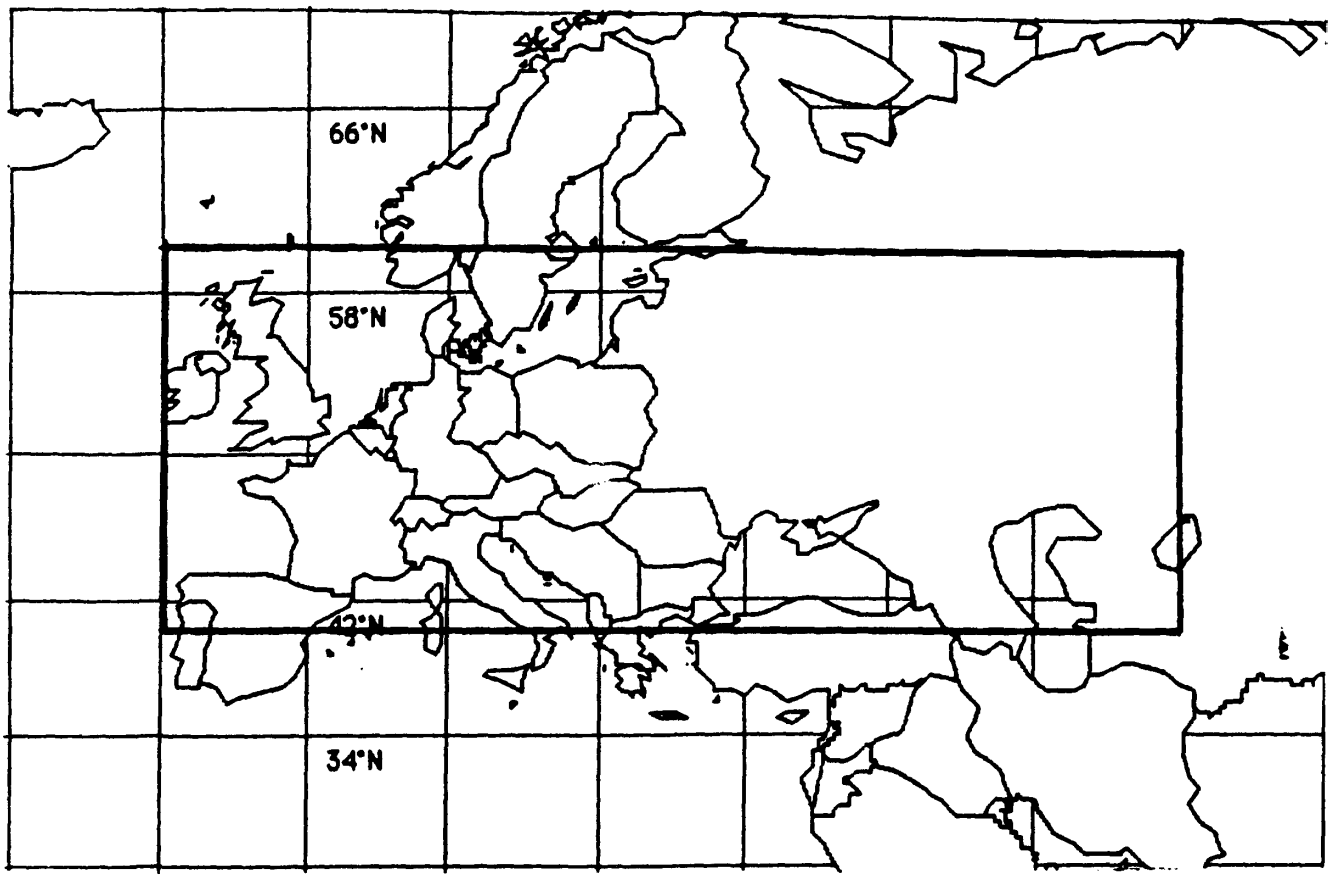

Figure 10. The area of Europe used in the regional gridpoint intercomparison study. At a 4° latitude by 5° longitude resolution, 52 land-based gridpoints are contained in this region.

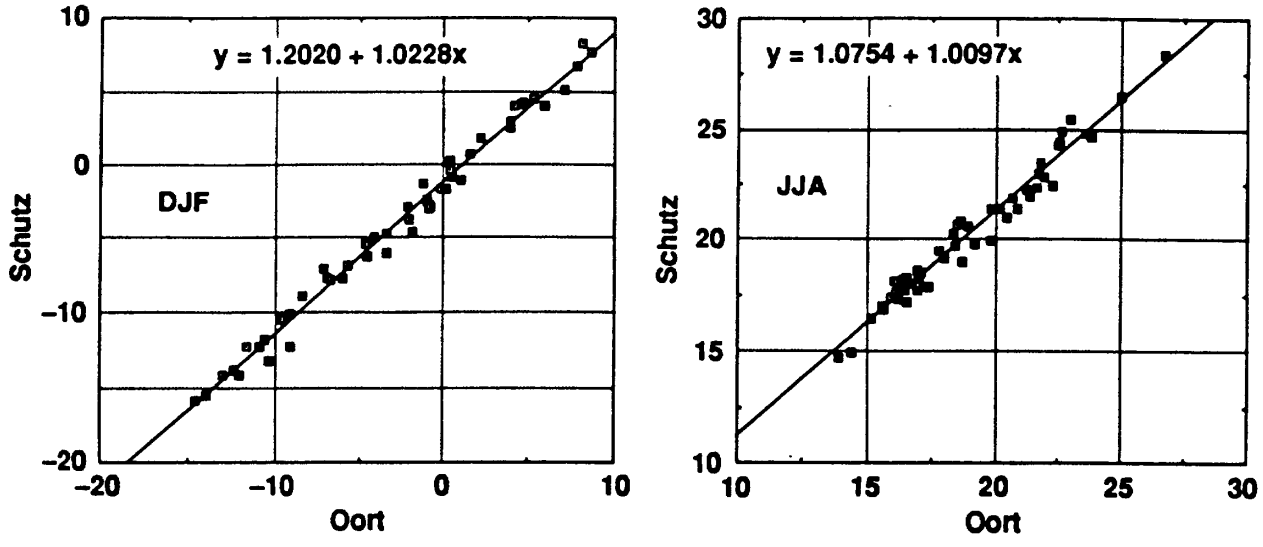

Figure 11. Seasonally averaged Dec/Jan/Feb and June/July/August temperatures from the observational data sets of Oort and Schutz and Gates. Each of the 52 points in each subplot is an individual land-based gridpoint in the area defined in Fig. 10.

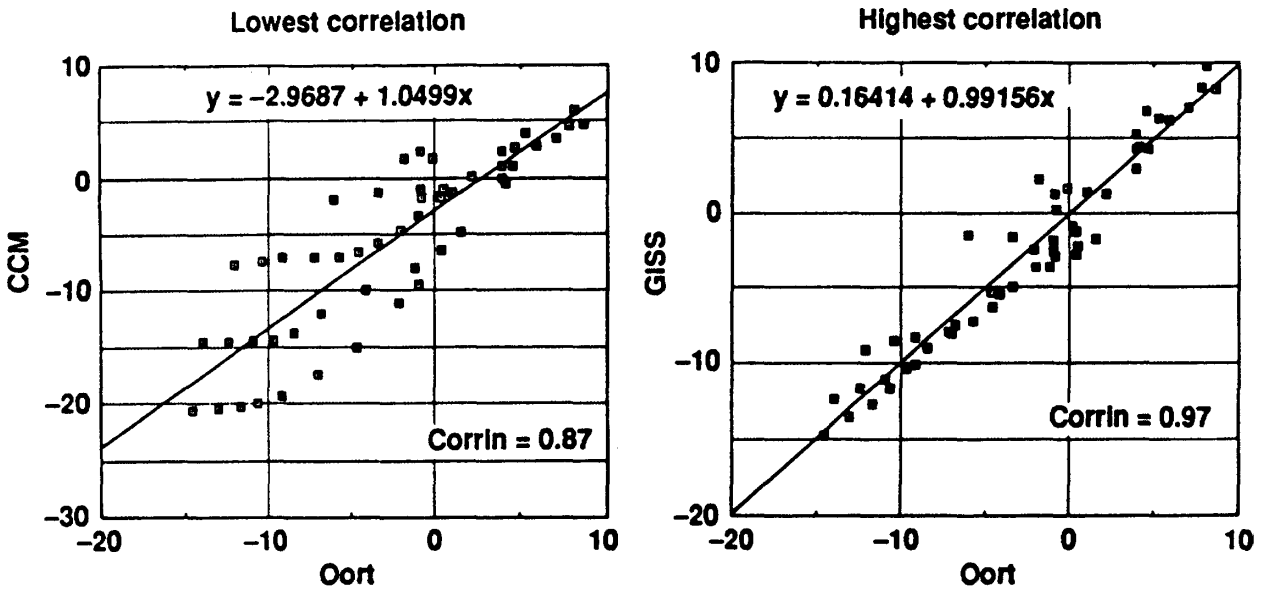

Figure 12. The lowest and the highest correlated GCM results for seasonally averaged Dec/Jan/Feb temperatures from the five GCMs and the observational data set of Oort. Each of the 52 points in each subplot is an individual land-based gridpoint in the area defined in Fig. 10.

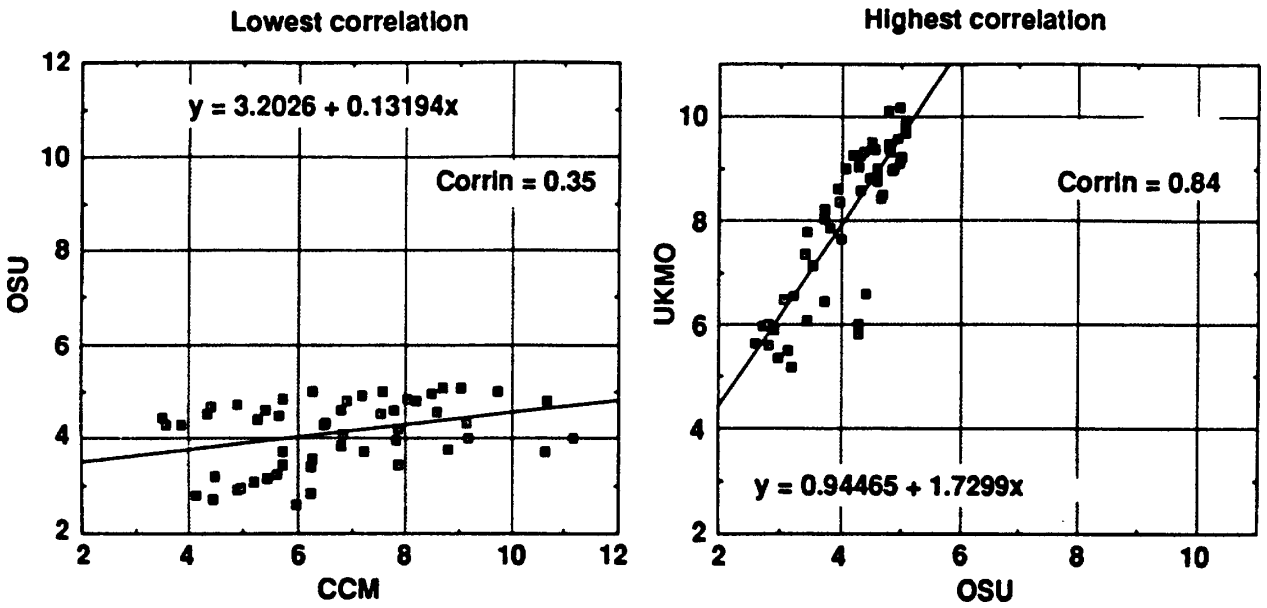

Figure 13. The lowest and the highest correlated pair of GCM results for seasonally averaged change in Dec/Jan/Feb temperatures from the five GCMs. Each of the 52 points in each subplot is the model prediction for change in temperature at an individual land-based gridpoint in the area defined in Fig. 10.